ELSEVIER

Journal of Alloys and Compounds 452 (2008) 384–388

Journal of ALLOYS AND COMPOUNDS

www.elsevier.com/locate/jallcom

Effect of heat-treatment on cobalt–molybdenum system

I. Kashif [a,*], A.A. Soliman [c], Z.M. El-Bahy [b]

[a] Physics Department, Faculty of Science, Al-Azhar University, Nasr City, Cairo, Egypt
[b] Chemistry Department, Faculty of Science, Al-Azhar University, Nasr City, Cairo, Egypt
[c] Physics Department, Faculty of Girls, Ain Shams University, Heliopoils, Cairo, Egypt

Received 25 June 2006; received in revised form 13 October 2006; accepted 28 October 2006
Available online 5 December 2006

Abstract

The binary oxide Co–Mo oxides were prepared by mixing the propagate amounts of aqueous cobalt nitrate and ammonium molybdate solutions at pH 5.0 to give ratio of Mo/Co = 1, followed by evaporation of water and by decomposition of the deposit at different temperatures from 200–900 °C. The obtained samples before and after heat-treatment were subjected to XRD and IR techniques to examine their structure. From both of them, it can be observed that, by increasing the temperature of heat-treatment the cobalt–molybdate oxide is strongly observed and cobalt–molybdate hydrate decreased. The lines characteristic for cobalt–molybdate hydrate is absented for heated sample at 900 °C indicating that cobalt–molybdate oxide is only oxide formed at this temperature.

The crystallization kinetic parameters were studied from DSC curves at different heating rates by using different methods. The crystallization process occurred with three mechanisms and bulk crystallization.

Keywords: Chemical synthesis; X-ray diffraction; Calorimetry

1. Introduction

Several investigations have been done for the catalytic decomposition of hydrogen peroxide in the presence of metal oxide catalysts [1–5]. This is due to the fact that catalytic activity of metal oxide is markedly affected by the addition of the other metal oxide.

Molybdenum carbonyls [6–10] and cobalt carbonyl [9–14] have been studied as possible alternative precursors for supported Mo and CoMo hydrotreating catalysts. The advantages of the carbonyl precursors are better dispersion; smaller surface particles and easier activation compared with the conventional catalysts [7,9].

Variation of property of Co_3O_4–MoO_3 binary oxide with its composition had been studied [5,15,16]. It was reported that, the addition of a small amount of molybdenum trioxide to cobalt oxide, caused remarkable changes in specific activity and apparent activation energy. According to their results, when the numbers of Co and Mo atoms are similar, molybdenum plays a more important role in the reaction than cobalt [16].

In the present work, the structure studies of the binary oxide sample of Co/Mo = 1 are made by using, XRD and IR techniques. DSC curves are used to study the crystallization kinetic parameters by using different methods and compared between these methods.

2. Experimental work

The chemicals used in this work are of AR grade quality. Stock solutions of cobalt nitrate [$Co(NO_3)_2 \cdot 6H_2O$] and ammonium molybdate [$(NH_4)_6Mo_7O_{24} \cdot 4H_2O$] were prepared. The binary system of Co–Mo mixed oxide have been prepared by the evaporation technique [1]. The appropriate amounts of cobalt nitrate and ammonium molybdate solutions are mixed to obtain the desired atomic ratio of Co/Mo = 1. Then, these solutions were evaporated in a water bath till dryness and the residues were dried in a furnace at 120 °C over night. Finally, these solid residues were heat-treated at 200–900 °C for 3 h.

The obtained samples before and after heat-treatment were subjected to X-ray diffraction by using Cu Kα radiation with a Ni filter and to infrared absorption spectra by using, IR Jasco 3500 FTIR spectrophotometer to throw light on their structure. DSC measurements were made by using Shimadzu 50 DSC to investigate the kinetic parameters for crystallization process.

---

* Corresponding author. Tel.: +20 2 4558035.
E-mail address: isnham@netscape.net (I. Kashif).

0925-8388/$ – see front matter © 2006 Elsevier B.V. All rights reserved.
doi:10.1016/j.jallcom.2006.10.154

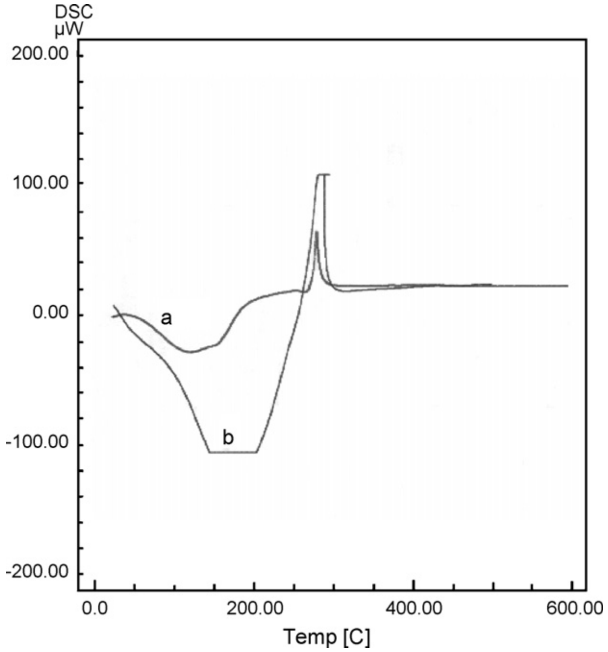

Fig. 1. DSC curves for the investigated sample: (a) at air furnace atmosphere and (b) at nitrogen furnace atmosphere.

3. Results and discussion

3.1. DSC measurements

3.1.1. -Effect of furnace atmosphere

The temperature for crystallization, T_c, and the maximum of the crystallization peak, T_p, were measured using non-isothermal DSC technique as a function of furnace atmosphere, e.g. nitrogen and air atmosphere. Fig. 1a and b shows the DSC curves for the investigated sample at air and nitrogen furnace atmosphere, respectively. It shows a difference between both of temperatures, T_c and T_p measured using both of atmospheres, nitrogen and air. It was found to be about 60 and 80 °C, respectively, at heating rate of 30 °C. This difference may be due to the air atmosphere helps the crystallization process and causes a decrease of T_c and T_p, but nitrogen flow had no effect on the crystallization process. The only change observed was the increased intensity of the heat flow as seen in Fig. 1b. It seems that nitrogen reacts with the sample itself and helps the liberation of heat. This agrees well with the results from IR spectra of molybdenum carbonyl surface when heated under nitrogen [16].

3.1.2. -Crystallization kinetics of the sample

Fig. 2 shows the non-isothermal DSC curves for the investigated sample at different heating rate, ϕ, up to 40 °C/min. It is clear that the exothermic peak becomes sharper and shifted to higher frequency as heating rate increases.

The theoretical basis for interpreting DSC results is provided by the formal theory of transformation kinetics as developed by special case of Johnson–Mehl–Avrami equation [17,18]:

$$x = 1 - \exp\{-(Kt)^n\}$$

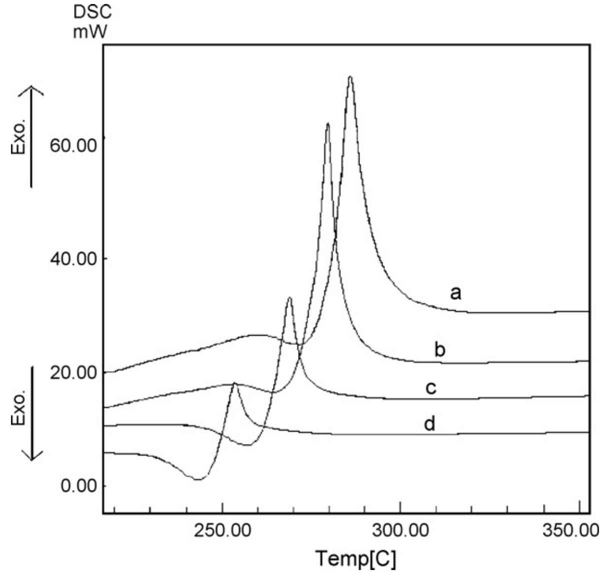

Fig. 2. DSC curves for the investigated sample: (a) 40 °C/min, (b) 30 °C/min, (c) 20 °C/min and (d) 10 °C/min.

where K is defined as the effective overall reaction rate, which is usually assigned Arrhenion temperature dependence as:

$$K = K_0 \ \exp\left(\frac{-E}{RT_p}\right)$$

where E is the effective activation energy describing the overall crystallization process and x is the volume fraction of crystallization. The fraction of crystallization at constant temperature for different heating rates is assumed to be proportional to the amount of heat evolved during crystallization which is proportional to the area under the exothermic, n, known as the Avrami exponent, is related to directionality of crystal growth. The value of n, can be determined from the slope of plotting the relation between $\ln[-\ln(1-x)]$ versus $\ln\phi$ as shown in Fig. 3 according the relation [19]:

$$\frac{d\ln[-\ln(1-x)]}{d\ln\phi} = n,$$

where ϕ is the heating rate.

The deduced value of n is equal about 3.6, which revealed that the crystallization process was occurred with three mechanisms and bulk crystallization growth [20].

The activation energy, E, of crystallization has been calculated by using different methods. These methods are Kissinger [21], Takhor [22], Augis–Bennett [23] and Ozawa–Chen [24,25] method that evaluated, E, from different thermograms held at different heating rates. The first three methods are based on the determination of the fraction of crystallization, x, for different heating rates using the dependence of peak crystallization temperature, T_p, on the heating rates, ϕ. While the last method (Ozawa–Chen) is based on the effect of heating rate, ϕ, on the temperature at which the crystallization fraction, x, is constant.

The method of Kissinger [21] for calculation of the activation energy for crystallization from the slope of the straight line which are plotted from the relation between $\ln(T_p^2/\phi)$ versus

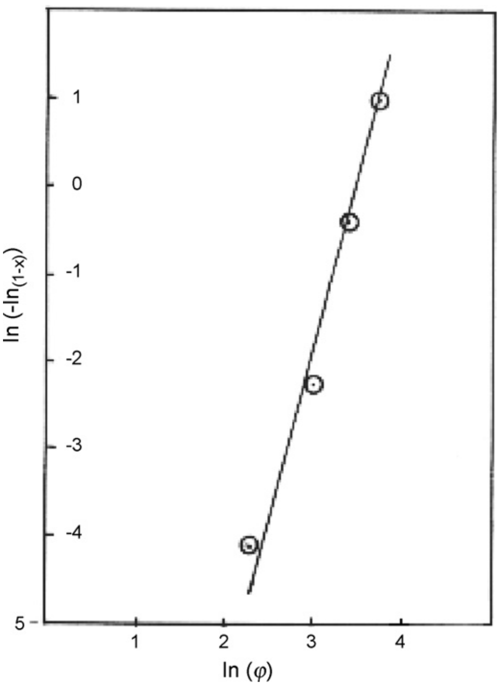

Fig. 3. The relation between $\ln[-\ln(1-x)]$ vs. $\ln\phi$.

$1/T_p$ for different heating rate as shown in Fig. 4a according to equation:

$$\ln\left(\frac{T_p^2}{\phi}\right)=\ln\left(\frac{E}{R}\right)-\ln A+\frac{E}{RT_p}$$

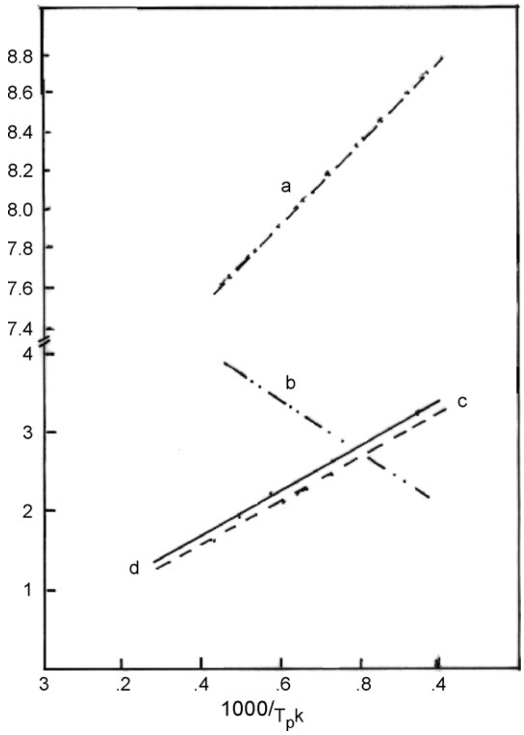

Fig. 4. The relation between: (a) $\ln(T_p^2/\phi)$ vs. $1/T_p$ (Kissinger's method), (b) $\ln\phi$ vs. $1/T_p$ (Takhor's method), (c) $\ln\{(T_p-T_0)/\phi\}$ vs. $1/T_p$ (Augis–Bennett's method) and (d) $\ln(T_p/\phi)$ vs. $1/T_p$ (Ozawa–Chen's method).

Table 1
The estimated values of the activation energy of crystallization for the investigated sample by using four different methods

Methods	E (kJ/mol)
Kissinger	17.488
Takhor	25.981
Augis–Bennett	26.131
Ozawa–Chen	23.636

where A is constant which depends on the material and R is the gas constant. The activation energy has been calculated and tabulated in Table 1.

Also, the activation energy was obtained by using Takhor's method [22] according to equation:

$$\ln\left[\frac{\phi}{T_p-T_0}\right]=\frac{1}{n}\ln\left[\frac{n}{n-1}\right]+\ln(K_0)-\frac{E}{RT_p}$$

where T_0 is the starting temperature of crystallization. Takhor studied the relation between $\ln\phi$ versus $1/T_p$ as shown in Fig. 4b, where assumed that $\ln(T_p-T_0)$ as a function which changes more slowly with heating rate than $1/T_p$. The deduced activation energy is summarized in Table 1.

By using Augis and Bennett's method [23] which considering the effect of the term $\ln(T_p-T_0)$ in the calculation of the activation energy according to equation:

$$\ln\left\{\frac{T_p-T_0}{\phi}\right\}=-\ln K_0+\frac{E}{RT_p}$$

Fig. 4c shows the relationship between $\ln(\Delta T/\phi)$ and $1/T_p$ from which the activation energy was calculated and tabulated in Table 1.

Finally, the Ozawa–Chen method [24,25] studied $\ln(T_p/\phi)$ versus $1/T_p$ at constant crystallization fraction according to equation:

$$\ln\left(\frac{T_p}{\phi}\right)=-\frac{1}{n\ \ln K_0}+\frac{E}{RT_p}$$

Fig. 4d shows this relationship for different heating rate from which the activation energy has been calculated and tabulated in Table 1.

From Table 1, it can be observed that the values of the activation energy of crystallization of the $CoMoO_4$ phase obtained by both Takhor and Augis–Bennett methods are reinforcing each other. And the activation energy values obtained from the Kissinger method to be much smaller than other values. The noticeable difference between the results obtained by these two models and those obtained by the Kissinger's method (*Kissinger method is commonly used which is one of the most used methods for crystallization kinetic studies. The activation energy of crystallization can be determined by using Kissinger equation*) could be attributed to the applicability of Kissinger equation to non-isothermal kinetics. And this activation energy is deduced without taking into account the crystallization mechanisms. In some cases, surface crystallization and bulk crystallization occur simultaneously. The Kissinger equation is valid only when crystal growth occurs on a fixed number of nuclei during crystallization process. Incorrect values for the activation energy can be obtained if a majority of the nuclei are formed during crystallization.

A comparison among all the above different calculated methods of the activation energy and its average value has been made. From which it can be deduced that all the used methods are valid to determine the activation energy with different accuracy. The most accurate method deduced according to this study is suggested to be Ozawa–Chen's method, since the minimum deviation from the average value is about 0.055%.

3.1.3. X-ray diffraction analysis

X-ray diffraction pattern of the investigated sample before and after heat-treatment at 200, 300, 400, 500 and 900 °C are shown in Fig. 5a–f. XRD pattern for the untreated sample shows the amorphously state of the sample. The heat-treated sample at 200–900 °C are shown in Fig. 5b–f. Most of the lines characteristic for $CoMoO_4$ hydrate observed in all heat-treated samples except the sample of heat-treated at 900 °C. But the intensity of the peak increased by increasing the temperature. At higher temperature of heat-treatment, the line characteristic for cobalt–molybdate [$CoMoO_4$] in addition to line of $CoMoO_4$ hydrates and line of MoO_3 [5]. For heat-treated at 900 °C, the strongest peak observed characteristic for cobalt–molybdenum oxide ($CoMoO_4$) only. This indicates that $CoMoO_4$ can be formed at higher temperature [5].

The absence of lines which characteristic for $CoMoO_4$ hydrate and MoO_3 in the diagram of sample heat-treated at 900 °C indicates that cobalt–molybdate is only mixed oxide formed at this high temperature.

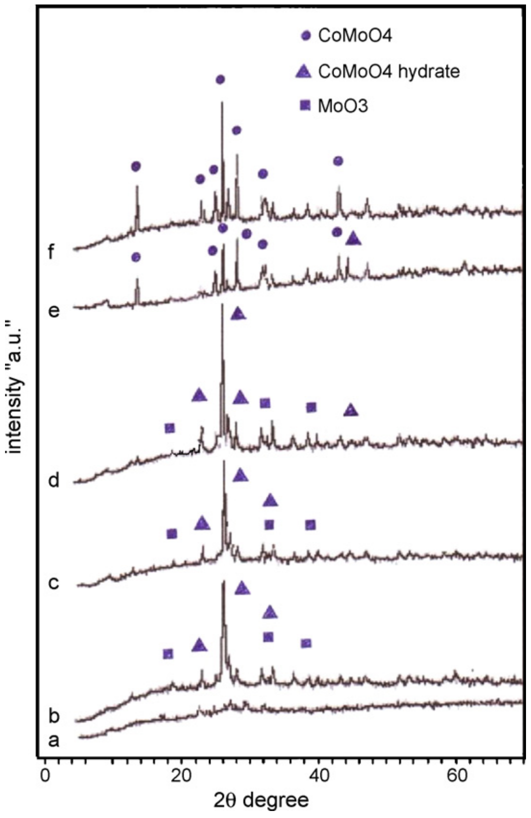

Fig. 5. XRD for heat-treated sample: (a) 200 °C, (b) 300 °C, (c) 400 °C, (d) 500 °C, (e) 700 °C and (f) 900 °C.

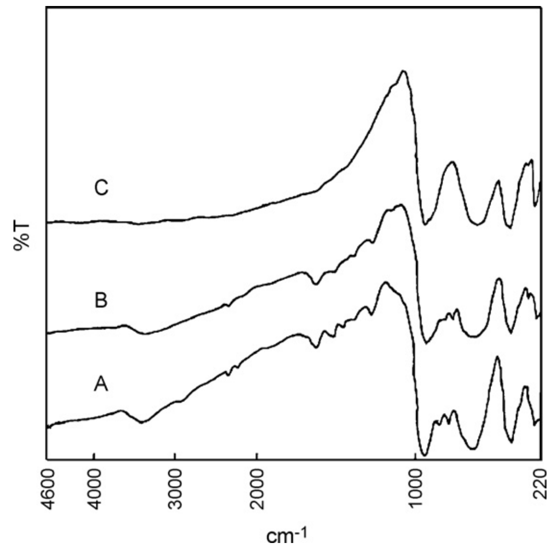

Fig. 6. IR spectra for: (A) untreated sample, (B) heat-treated sample at 500 °C and (C) heat-treated sample at 900 °C.

3.1.4. Infrared analysis

The IR spectra of Co_3O_4 and MoO_3 are reported previously [26]. It was reported that the absorption bands of Co_3O_4 were at 655, 635, 562, 460 and 350 cm^{-1}. For MoO_3 were reported at 660, 375, 300 and 850 cm^{-1} which assigned to Mo$\cdots$O stretching vibration and at 1000 cm^{-1} was assigned to Mo$\cdots$O stretching vibration in MoO_3 [15].

Fig. 6A–C shows the spectra of the sample untreated and heat-treated at 500 and 900 °C, respectively. Several absorption bands were observed for the untreated sample. The absorption bands at higher wavenumber decreased with increasing the heat-treatment and gradually disappeared at treated temperature 900 °C. Five absorption bands were observed at lower wavenumber which are at 940, 844, 785, 680 and 420 cm^{-1}. The three absorption bands at 940, 844 and 785 cm^{-1} were detected in all treated and untreated samples. These bands are assigned to $CoMoO_4$ [26,15,5]. The other band at 680 is due to Mo–O–Mo in MoO_6 group [26]. The band at 420 cm^{-1} may be attributed to bending vibration of $CoMoO_4$ structure [27].

4. Conclusions

From the experimental results, the following conclusions can be drawn:

(1) The XRD measurements showed that the investigated cobalt–molybdenum system crystallizes formed $CoMoO_4$ phase.
(2) DSC results showed a difference between both of temperatures; T_c and T_p measured using both of atmospheres, nitrogen and air.
(3) The crystallization behavior of samples has been investigated under non-isothermal conditions. After heat-treated at

900 °C, the Avrami constant for the samples was 3.6 and the activation energy of crystallization was 23.636 kJ mol^{-1}. It indicates bulk crystallization.

(4) The activation energy, *E*, of crystallization has been calculated by using different methods. Values of the activation energy of crystallization of the $CoMoO_4$ crystalline phase obtained by both Takhor and Augis–Bennett methods are reinforcing each other. A comparison among all the above different calculated methods of the activation energy and its average value has been made. The most accurate method deduced according to this study is suggested to be Ozawa–Chen's method, since the minimum deviation from the average value is about 0.055%.

References

[1] Y. Moro-Oka, S. Tan, A. Ozaki, J. Catal. 12 (3) (1968) 291.
[2] F.I. Zidan, M. Wasel, M. El-Wardani, J. Serb., Chem. Soc. 54 (8) (1989) 425.
[3] J.R. Goldstein, A.C.C. Tseung, J. Catal. 32 (3) (1974) 452.
[4] V. Mucka, Collec. Czchosllov. Chem. Commun. 49 (1984) 2231.
[5] F.I. Zidan, R.A. Ali, Z.M. El-Bahy, I. Kashif, Egypt. J. Appl. Sci 12 (1997) 4.
[6] A. Ishihara, K. Shirouchi, T. Kabe, Chem. Lett. 589. (1993).
[7] A. Maezawa, M. Kitamura, K. Wakamoto, Y. Okamoto, T. Imanaka, Chem. Express 3 (I) (1988).
[8] Y. Okamoto, A. Maezawa, H. Kane, T. Imanaka, J. Mol. Catal. 52 (1989) 337.
[9] Y. Okamoto, M. Odawara, H. Onimatsu, T. Imanaka, Ind. Eng. Chem. Res. 34 (1995) 3703.
[10] M. Stencel, L.E. Makovsky, R.E. Tischer, G.A. Melson, Proc. Int. Conf. (August) (1983) 15–19.
[11] T.R. Halbert, T.C. Ho, E.I. Stiefel, R.R. Chianelli, M. Daage, J. Catal. 130 (1) (1991) 116.
[12] F. Mauge, A. vallet, J. Bachelier, J.C. Duchet, J.C. Lavalley, Catal. Lett. 2 (1989) 57.
[13] F. Mauge, J.C. Lavalley, J. Catalysis 137 (1992) 69.
[14] F. Mauge, A. Vallet, J. Bachelier, J.C. Duchet, J.C. Lavalley, J. Catal. 162 (1) (1996) 88.
[15] Y. Moro-Oka, S. Tan, A. Ozaki, J. Catal. 17 (2) (1970) 125.
[16] M. Kurhinen, T.A. Pakkanen, J. Appl. Catal. A 192 (2000) 97.
[17] C.S. Roy, U. Huang, D.E. Day, J. Am. Cerm. Soc. 74 (1991).
[18] S. Dingkun, W. Kaiitai, H. Xihuai, C. Youxin, B. Jinhua, J. Non-Cryst. Solids 52 (1982) 151.
[19] T. Ozawa, Polymer 12 (1971) 150.
[20] P.C. Mitchell, F. Trifira, J. Chem. Soc., (A) 318 (1970).
[21] H.G. Kissingor, Anal. Chem. 29 (1957) 1702.
[22] R.L. Takor, Am. Ceram. Soc. 166 (1972).
[23] J.A. Augis, J.E. Bennett, J. Therm. Anal. 13 (1978) 283.
[24] T. Ozawa, Bull. Chem. Soc., Jpn. 38 (1965) 1881.
[25] H.S. Chen, J. Non-Cryst. Solids 27 (1978) 257.
[26] F.I. Zidan, M.S. El- Agha, J. Fac. Educ. (1988).
[27] Y.Y. Kim, D.H. Lee, T.Y. Kwon, S. Hopark, J. Solid State Chem. 112 (1994) 376.